

An Approach to Sensorless Operation of the Permanent-Magnet Synchronous Motor Using Diagonally Recurrent Neural Networks

Todd D. Batzel and Kwang Y. Lee, *Fellow, IEEE*

Abstract—Due to the drawbacks associated with the use of rotor position sensors in permanent-magnet synchronous motor (PMSM) drives, there has been significant interest in the so-called rotor position sensorless drive. Rotor position sensorless control of the PMSM typically requires knowledge of the PMSM structure and parameters, which in some situations are not readily available or may be difficult to obtain. Due to this limitation, an alternative approach to rotor position sensorless control of the PMSM using a diagonally recurrent neural network (DRNN) is considered. The DRNN, which captures the dynamic behavior of a system, requires fewer neurons and converges quickly compared to feedforward and fully recurrent neural networks. This makes the DRNN an ideal choice for implementation in a real-time PMSM drive system. A DRNN-based neural observer, whose architecture is based on a successful model-based approach, is designed to perform the rotor position estimation on the PMSM. The advantages of this approach are discussed and experimental results of the proposed system are presented.

Index Terms—Motor drives, neural networks, observers, permanent magnet motors, sensorless operation.

I. INTRODUCTION

IN high-performance permanent-magnet synchronous motor (PMSM) applications, high resolution rotor angle information is required to operate the machine efficiently and to generate smooth torque. A resolver or encoder attached to the shaft of the rotor is typically used to supply this position feedback. These high resolution position sensors add length to the machine, raise system cost, increase rotor inertia and require additional cabling. The desire to eliminate the rotor position sensor from PMSM applications has resulted in the development of several techniques for sensorless operation [1]–[6]. In general, the techniques for sensorless control of the PMSM include open-loop flux estimators using the stator currents and voltages, third harmonic voltage-based position estimators, back electromotive-force (emf) waveform detection methods, and observers and rotor angle estimators based on position-dependent stator inductance variation.

The flux linkage estimation method [1] integrates the phase voltage minus the stator resistance drop to estimate the angle of

the flux linkage space vector. This angle is then used to produce the appropriate stator current references. This method, however, suffers at low speeds where integrator drift is a problem. Furthermore, estimation accuracy is highly sensitive to variations in the stator resistance, which is known to be temperature dependent.

A technique that monitors the third harmonic voltage to obtain the rotor angle has been developed in [2]. This technique is applicable to the brushless dc machine with trapezoidal back emf waveshape, but is of little relevance to the PMSM, which normally has a sinusoidal airgap flux distribution.

In the waveform detection techniques such as in [3], a specific characteristic of the back emf is exploited to determine the rotor position. These methods are simple and may be implemented using low-cost components, but accurate determination of the rotor angle is difficult because of the required low-pass filtering and the low amplitude of the back emf at low speeds. These techniques are more applicable to the brushless dc motor, where an open phase voltage may easily be measured.

The pioneering work in [4] implemented a model-based observer to determine the rotor angle. This observer, however, was found to be sensitive to mechanical parameters such as load torque, viscous and damping friction and inertia—parameters that are often changing dynamically or are unknown. In [5], the dependency on the mechanical parameters is removed in an observer-based approach, but the need for an electrical model of the machine remains.

For a salient rotor PMSM application, the position-dependent inductance variation can be monitored to derive the rotor angle [6]. This method, however, is unusable for the many machines that are constructed with surface-mounted permanent magnets in the rotor.

The increasing role of the artificial neural network (ANN) in a wide variety of engineering applications has spurred interest in its application to power electronics and motor drive systems. The artificial neural network (ANN) has several attractive characteristics that justify this interest, including a parallel distributed structure, ability to learn and identify nonlinear dynamics, ability to generalize and adaptivity. These characteristics suggest the enormous potential of the ANN in motor drive systems, including the sensorless PMSM.

A frequently used neural-network structure is the feedforward ANN. The drawbacks to using the feedforward ANN in real-time motor control applications include its static mapping characteristic, the requirement for a large number of neurons, and a long training time. Often, a tapped delay line is used with

Manuscript received April 12, 2002; revised April 24, 2002. This work was supported in part by the Office of Naval Research under Grant N00014-00-G-0058/007.

T. D. Batzel is with the Department of Computer Science and Engineering, Penn State Altoona, Altoona, PA 16601 USA (e-mail: tdbl20@psu.edu).

K. Y. Lee is with the Department of Electrical Engineering, Pennsylvania State University, University Park, PA 16802 USA (e-mail: kwanglee@psu.edu).

Digital Object Identifier 10.1109/TEC.2002.808386

the feedforward ANN to remove the static mapping restriction and obtain a dynamic mapping. This approach requires that the order of the system dynamics be known in advance to choose a suitable ANN structure.

Recently, the diagonally recurrent neural network (DRNN) with dynamic structure was introduced [7] where self-feedback of the hidden neurons ensures that system dynamics may be captured without the tapped delay approach. In addition to its dynamic mapping capabilities, the DRNN requires fewer neurons, is more easily implemented in real-time systems, and converges quickly compared to feedforward and fully recurrent ANN structures [7]. Thus, a new approach for neural observation of the PMSM rotor position using a DRNN topology is considered.

II. MODEL-BASED OBSERVER APPROACH

Assuming that the mathematical model for the PMSM is available, in [5], sensorless control of the PMSM was achieved using the system model and a Luenberger observer. In this work, a separation of time scales is used to yield a linear system model for the PMSM. With this approach, the fast electrical dynamics are represented by

$$\dot{x} = A_\omega x + Bu \quad (1)$$

$$y = Cx \quad (2)$$

where the state, input, and output vectors are given by

$$x = [x_1 x_2 x_3 x_4]^T = [\lambda_\alpha \lambda_\beta \cos \theta \sin \theta]^T \quad (3)$$

$$u = [u_1 u_2]^T = [v_\alpha v_\beta]^T \quad (4)$$

$$y = [y_1 y_2]^T = [i_\alpha i_\beta]^T. \quad (5)$$

In (1)–(5), $\lambda_{\alpha,\beta}$, $v_{\alpha,\beta}$ and $i_{\alpha,\beta}$ represent the flux linkage, terminal voltage, and phase current, respectively, of the fictitious windings in the two phase stationary reference frame. The symbol θ represents the rotor angle in electrical radians.

The state space matrices are given by

$$A_\omega = \begin{bmatrix} -\tau & 0 & \sqrt{\frac{3}{2}}\lambda_m\tau & 0 \\ 0 & -\tau & 0 & \sqrt{\frac{3}{2}}\lambda_m\tau \\ 0 & 0 & 0 & -\omega_e \\ 0 & 0 & \omega_e & 0 \end{bmatrix} \quad (6)$$

$$B = \begin{bmatrix} 1 & 0 \\ 0 & 1 \\ 0 & 0 \\ 0 & 0 \end{bmatrix}$$

$$C = \begin{bmatrix} \frac{\tau}{R} & 0 & -\sqrt{\frac{3}{2}}\frac{\tau\lambda_m}{R} & 0 \\ 0 & \frac{\tau}{R} & 0 & -\sqrt{\frac{3}{2}}\frac{\tau\lambda_m}{R} \end{bmatrix} \quad (7)$$

$$\tau = \frac{R}{L_l + \frac{3}{2}L_{ss}}.$$

The term ω_e represents the angular velocity of the rotor shaft in electrical radians per second and λ_m is the permanent-magnet flux constant. The symbols R , L_{ss} , and L_l

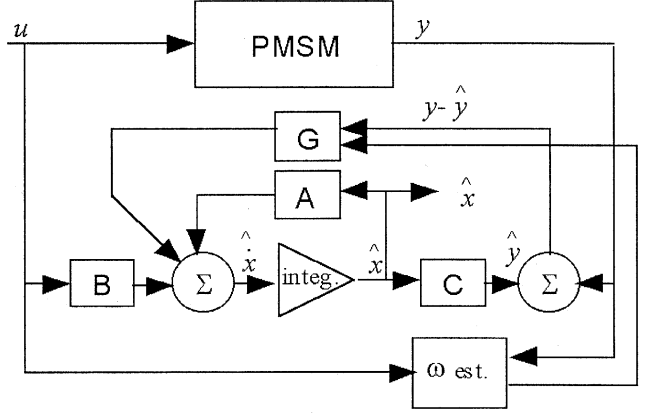


Fig. 1. Rotor position observer for PMSM using Luenberger observer.

represent the phase resistance, self-inductance and leakage inductance, respectively, while τ is the electrical time constant of the machine. The subscript ω associated with the A matrix indicates that this matrix varies with the angular velocity of the rotor and is therefore a time-varying system matrix.

From (6), the fast electrical model is dependent on the slowly varying angular velocity, which is considered to be a parameter in the fast time scale. In a sensorless application, the angular velocity must also be estimated. This is accomplished by considering the back emf to be a space vector. From this viewpoint, the magnitude and polarity of the velocity can be determined from magnitude and direction of rotation, respectively, of the rotating back emf vector [5]

$$\begin{aligned} \hat{\omega}_e &= \text{sign}(\theta_{emf}(k) - \theta_{emf}(k-1)) |\hat{\omega}_e| \\ |\hat{\omega}_e| &= \frac{\left[(v_\alpha - Ri_\alpha)^2 + (v_\beta - Ri_\beta)^2 \right]^{1/2}}{\sqrt{\frac{3}{2}}\lambda_m} \\ \theta_{emf}(k) &= \tan^{-1} \left(\frac{Ri_\alpha(k) - v_\alpha(k)}{v_\beta(k) - Ri_\beta(k)} \right) \end{aligned} \quad (8)$$

The result is the system shown in Fig. 1 in which two separate observers—angular velocity and rotor position estimators—are used to achieve the objective of rotor position estimation. The observer gain matrix G shown in Fig. 1 is selected to achieve the required convergence characteristics. A tremendous advantage to this approach is that it does not require any knowledge of the mechanical parameters such as load torque, friction, and rotor inertia which are often difficult to obtain, or are changing with time.

Despite the independence from the mechanical variables, this model-based approach requires some knowledge of the PMSM structure and electrical parameters, which in some situations is not readily available or difficult to obtain. Back EMF waveshape and saliency characteristics for a PMSM are not always available from the manufacturer. Due to this potential dilemma, a new approach should be considered—the neural observer. Due to the many advantages of the approach outlined before, the DRNN-based neural observer is based in principal on the structure of the Luenberger observer developed in [5].

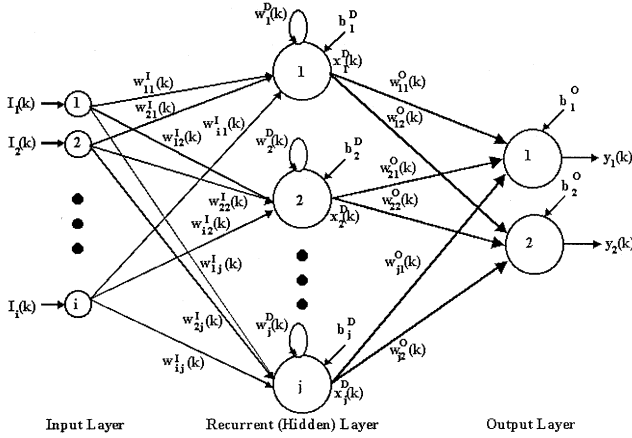


Fig. 2. DRNN structure.

III. DIAGONAL RECURRENT NEURAL NETWORK

A. DRNN Structure

The structure of the DRNN is shown in Fig. 2 for a system with i inputs, j recurrent neurons, and two output neurons. In a DRNN, the only recurrent connections that are allowed are self-recurrent connections in the hidden layer, where the recurrent connections are assumed to incorporate a delay. In the absence of the self-recurrent connections, the architecture becomes a feedforward network.

The generated output of the m th output layer neuron and j th recurrent layer neuron are given in (9) and (10), respectively, and the sum of inputs to recurrent neurons is given in (11)

$$y_m(k) = \sum_j w_{jm}^O x_j(k) \quad (9)$$

$$x_j(k) = f(S_j(k)) \quad j = 1, 2, \dots, j \quad (10)$$

$$S_j(k) = w_j^D x_j(k-1) + \sum_i w_{ij}^I I_i(k) \quad j = 1, 2, \dots, j. \quad (11)$$

In (11), $I_i(k)$ represents the i th input to the neural network at discrete time k . The weight matrices w_{ij}^I , w_j^D , and w_{jm}^O represent the input layer weight (connecting input i and recurrent neuron j), the weights of the self feedback loop for neuron j and the output layer weight from recurrent neuron j to the m th output neuron, respectively. The superscripts I , D , and O associated with the weights are used to indicate the input, diagonally recurrent, and output layers, respectively. The function $f(\cdot)$ in (10) is the commonly used bipolar tansigmoid transfer characteristic where

$$f(x) = \frac{2}{1 + \exp(-x)} - 1. \quad (12)$$

The bias terms shown in Fig. 2 for the recurrent and output layer neurons are also included in (9) and (11) by considering the bias as a weighted connection with unity input. That is, $w_{0m}^O = b_m^O$ and $x_0(k) = 1$ in (9) while $w_{0j}^D = b_j^D$ and $I_0(k) = 1$ in (11).

B. Dynamic Backpropagation

The goal of backpropagation is to minimize a cost function, which is normally selected to be the squared error between the actual ANN output and the desired value. Let the training set consist of the desired output of the m th output layer neuron $d_m(k)$ and the input pattern $I_i(k)$. With the desired output defined, the error corresponding to output neuron m is represented by

$$e_m = d_m(k) - y_m(k) \quad (13)$$

and the total cost function to be reduced during the training process is

$$E = \frac{1}{2} \sum_m e_m^2. \quad (14)$$

A training algorithm applicable to the DRNN using dynamic backpropagation has been developed in [7] and [8]. In the following, these results are extended for the case of multiple output neurons. As shown in [7], a rule for continuous updating of the weights is

$$w(n+1) = w(n) + \eta \left(-\frac{\partial E}{\partial w} \right) + \beta (\Delta w(n-1)) \quad (15)$$

where η represents the learning rate, n is the iteration index, β is a momentum term, and $\Delta w(n-1)$ represents the change in weight w at the previous iteration. The momentum term is included to help ensure that the error converges to a global minimum. To apply (15) to the DRNN training, any specific input, output, or recurrent weight may be substituted for the symbol w . The remaining results required to implement dynamic backpropagation are summarized in (16)–(20)

$$-\frac{\partial E}{\partial w_{jm}^O} = e_m(k) x_j(k) \quad (16)$$

$$-\frac{\partial E}{\partial w_j^D} = P_j(k) \sum_m w_{jm}^O e_m \quad (17)$$

$$\frac{\partial E}{\partial w_{ij}^I} = Q_{ij}(k) \sum_m w_{jm}^O e_m \quad (18)$$

$$P_j(k) = f'(S_j) (X_j(k-1) + w_j^D P_j(k-1)) \quad (19)$$

$$Q_{ij}(k) = f'(S_j) (I_i(k) + w_j^D Q_{ij}(k-1)) \quad (20)$$

Note that the output layer weights are influenced by only the error at the output neuron to which the weight connects. For the recurrent and input layer weights, however, the error for each neuron in the output layer contributes to the weight update.

IV. DRNN-BASED ROTOR POSITION ESTIMATION

Based on a separation of time scales introduced in the preceding section, the DRNN-based neural observer is now developed. Like the Luenberger approach previously outlined, the system inputs to the proposed DRNN-based rotor position observer structure are the stator voltages and currents. Similar to the model-based method, the neural rotor position estimation

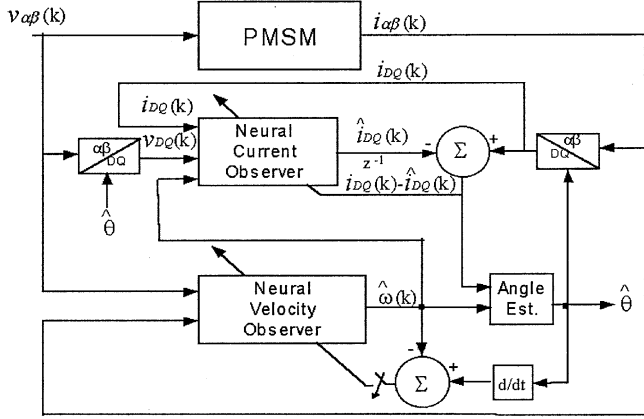


Fig. 3. DRNN-based neural observer for PMSM rotor angle.

process shown in Fig. 3 is separated into stator current, angular velocity, and rotor position estimators.

A. Description of Neural-Based Rotor Angle Observer

1) *Neural Current Observer*: The neural current observer included in the structure of Fig. 3 is used to map the estimated angular velocity $\hat{\omega}$ and the applied terminal voltage $v_{d,q}$ to the estimated stator current $\hat{i}_{D,Q}$. Since the rotor position is not directly measurable in a sensorless drive, machine variables such as the stator current must be represented in the estimated rotating reference frame. The actual d-q reference frame, which is fixed to the rotor and its relation to the estimated D-Q reference frame, is shown in the space vector diagram of Fig. 4. Transforming the terminal quantities from the stationary three-phase reference frame implies the use of the well-known Park transformation [9] using the estimated rotor angle $\hat{\theta}$. The PMSM model transformed into the rotating d-q reference frame is

$$\begin{bmatrix} v_d \\ v_q \end{bmatrix} = \begin{bmatrix} R + pL_d & -\omega_e L_q \\ \omega_e L_d & R + pL_q \end{bmatrix} \begin{bmatrix} i_d \\ i_q \end{bmatrix} + \sqrt{\frac{3}{2}} \lambda_m \omega_e \begin{bmatrix} 0 \\ 1 \end{bmatrix} \quad (21)$$

where p represents the differential operator and $v_{d,q}$ and $i_{d,q}$ represent the terminal voltages and currents, respectively, in the reference frame fixed to the rotor. The terms L_d and L_q in (21) represent the stator inductance in the direct and quadrature axis, respectively, and are equal in a round-rotor machine, so that $L_d = L_q = L_l + (3/2)L_{ss}$.

The neural current observer has no knowledge of the angular difference $\Delta\theta$ between the d-q and D-Q axes, and therefore, the measured current must be resolved into its components in the estimated reference frame ($i_{D,Q}$), as shown in Fig. 4. Thus, the DRNN is trained to estimate the stator current $\hat{i}_{D,Q}$. With the assumption that the actual and estimated reference frames are collinear, this mapping can be represented mathematically by

$$\begin{aligned} \hat{i}_D (R + pL_d) &= v_D + L_q \hat{\omega}_e i_Q \\ \hat{i}_Q (R + pL_q) &= v_Q - L_d \hat{\omega}_e i_D - \sqrt{\frac{3}{2}} \lambda_m \hat{\omega}_e \end{aligned} \quad (22)$$

where $\hat{i}_{D,Q}$ and $i_{D,Q}$ are the estimated and measured currents, respectively, in the estimated reference frame. The output of the

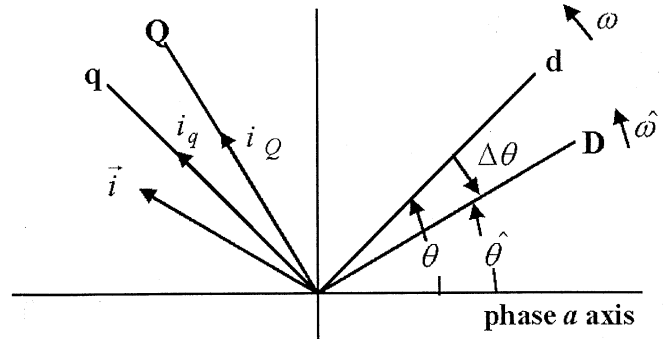


Fig. 4. Space vector diagram of PMSM in the rotating reference frame.

neural current observer is compared with the actual measured currents to yield the estimation error

$$e_{D,Q}(k) = i_{D,Q} - \hat{i}_{D,Q}. \quad (23)$$

The estimation error obtained by (23) is backpropagated to the current estimator DRNN, where the backpropagation algorithm described previously is used to adjust the connection weights.

2) *Neural Velocity Observer*: The neural velocity observer shown in Fig. 3 is used to map input voltage and current to the estimated PMSM angular velocity. The recurrent structure of the DRNN allows the velocity to be estimated from these inputs by learning the dynamics given in (8). Adaptive online correction to the neural velocity observer weights is generated from the velocity estimation error. A velocity estimation error is attainable despite the lack of a sensor because over a sufficiently long time period, the time derivative of the estimated rotor angle approaches the actual angular velocity. Thus, in steady state, an indication of the velocity estimation error is available and the neural velocity observer is trainable online under certain operating conditions.

It should be noted that since velocity changes much slower than the electrical dynamics of the current observer, the velocity observer may be updated at a rate much slower than the fast current observer. This aspect of the velocity estimator offers advantages in a real-time computing system.

3) *Position Estimation Correction*: In Fig. 3, the angle estimation block generates rotor angle by integrating the estimated angular velocity, with adjustment derived from the current estimation error given in (23). This process is similar to the operation of the observer gain matrix G used in the model-based approach, which corrects states x_3 and x_4 in (3) from the current estimation error. The usefulness of the current estimation errors to correct the position estimate can be demonstrated by the transformation of (21) into the estimated reference frame, which yields

$$\begin{bmatrix} v_D \\ v_Q \end{bmatrix} = \begin{bmatrix} R + pL_d & -\omega_e L_q \\ \omega_e L_d & R + pL_q \end{bmatrix} \begin{bmatrix} i_D \\ i_Q \end{bmatrix} + \sqrt{\frac{3}{2}} \lambda_m \omega_e \begin{bmatrix} \sin(\Delta\theta) \\ \cos(\Delta\theta) \end{bmatrix}. \quad (24)$$

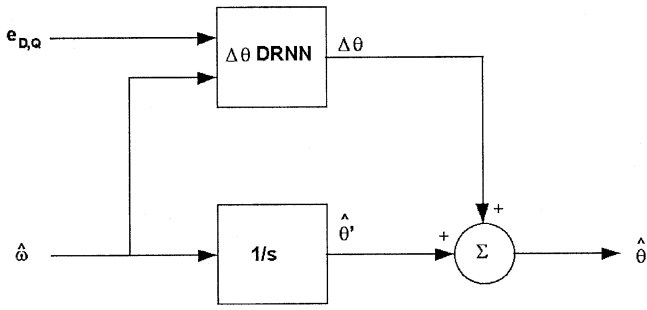


Fig. 5. Rotor angle estimation and correction block.

Comparing (22) and (24) and assuming a small angular difference $\Delta\theta$ gives

$$\begin{aligned} (R + pL_d) e_D &= \sqrt{\frac{3}{2}} \lambda_m \omega_e \Delta\theta \\ (R + pL_q) e_Q &= -\sqrt{\frac{3}{2}} \lambda_m (\omega_e - \hat{\omega}_e)' \end{aligned} \quad (25)$$

where e_D and e_Q are the current estimation errors defined in (23). Clearly, from (25), information regarding the angle estimation error is included in the current estimation error quantities, which suggests the position estimation strategy shown in Fig. 5.

B. DRNN Topology for Rotor Position Observer

Through experimentation, 15 neurons in the hidden recurrent layer were found to produce good results for the neural current observer. This number was selected to produce fast convergence and robust dynamic capturing capabilities. The output layer contains two neurons—one for each of the direct and quadrature axis current estimates.

Both the velocity and position estimation DRNN use five neurons in the hidden layer. In both cases, the output layer consists of a single neuron. The recurrent and output layers neurons for each of the three DRNN estimators use a tansigmoid and linear transfer functions, respectively.

C. DRNN Observer Training

The goal of the DRNN training process is to minimize the rotor position estimation error and to learn the machine dynamics. The proposed DRNN-based system was trained in two steps: offline training in which the dynamics of the PMSM are learned and online training where the adaptation of PMSM parameters is achieved.

1) *Offline Training:* The offline training process starts with a random initialization of the weights in each layer. Weights are normalized based on the expected range at the input neurons. The first set of training data consists of steady-state motoring in each direction with a constant load, in which case the rotor velocity is the constant synchronous speed. For each training iteration, the DRNN output is compared to its target. The resulting error function is then used with the dynamic backpropagation algorithm to adjust the weights of the DRNN. After the sum-squared error for the first set of training data converges to a predetermined threshold, additional training data consisting of

various speeds and load torques are slowly introduced one at a time. The offline training process is completed when the training data set consists of the entire range of operation for the motor under consideration and the sum-squared error meets the goal.

Each of the three DRNN neural estimators was first trained offline by using dynamic backpropagation. The neural current and velocity estimators are first trained, followed by the position estimator. The input vector to the current estimator DRNN consists of the stator voltages and rotor angular velocity, while the target vector is the actual stator current vector. The velocity estimation DRNN uses the stator voltage and current vectors as the inputs and the actual rotor velocity as the target vector. The position estimation DRNN uses the rotor velocity and current estimation errors as its inputs and the actual rotor angle as the target. For the offline training, the actual rotor angle and velocity were both obtained from a hollow shaft encoder temporarily attached to the shaft of the PMSM.

For the current estimator DRNN, approximately 6500 training iterations at a constant learning rate of .05 produced the weights used to perform system simulations. Significantly fewer iterations were required by both the velocity and position estimation DRNN.

2) *Online Training:* Much like state feedback correction is necessary in the model-based approach, adaptive correction of the DRNN weights is important in the neural estimator. Online training is performed to account for the inevitable parameter drift associated with operating temperature fluctuations.

For the DRNN current estimator, adaptive correction is achieved much like the offline training, with the exception that estimated rotor velocity is used as an input to the DRNN since actual velocity is not available in the real system. The velocity estimator may be trained online during periods of steady-state operation. In steady state, the time derivative of the estimated rotor angle approaches the actual velocity over a sufficient period of time. Thus, under steady-state operating conditions, the actual velocity determined from the estimated rotor angle can be used to adjust the weights of the velocity estimator online. Online training of the position estimation DRNN was not used, since the actual rotor angle is not available in a sensorless system.

D. Experimental Results

After the training of the DRNN, some test patterns were applied to the system to evaluate the effectiveness of the training process. The performance is tested under various steady-state and transient conditions.

Fig. 6 shows the DRNN observer performance at relatively high speed with a load equal to half-rated torque. In this experiment, an initial angle estimation error of 30 electrical degrees was intentionally introduced to the system. As demonstrated in the figure, the error is quickly corrected and the angle estimation error quickly approaches zero.

In Fig. 7, the robustness of the system to load torque variations is examined. For this experiment, a fast load change is imposed on the system. The results of this experiment demonstrate that the proposed system performs well under such load changes. This is the expected result, since the neural observer is patterned after the model-based approach, which was shown

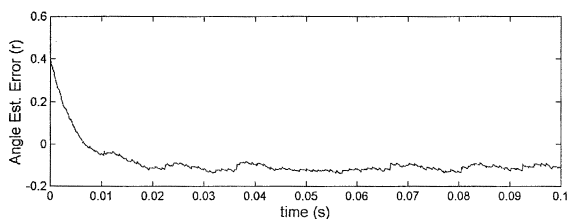


Fig. 6. NN estimation accuracy at 800 r/min, 5 ft-lb.

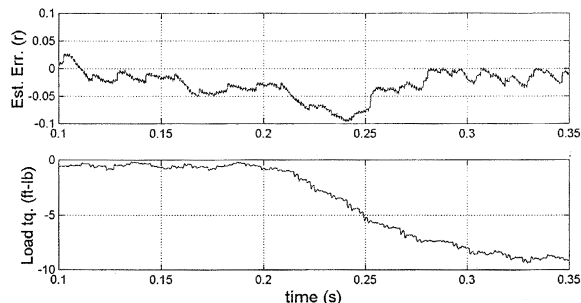


Fig. 7. NN estimation accuracy—400 r/min, fast load change.

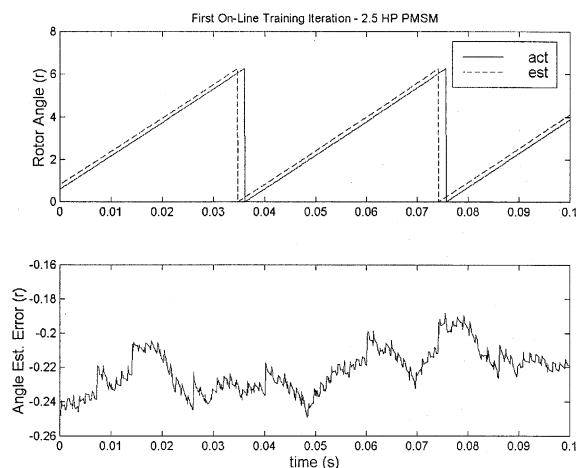


Fig. 8. Online training of 2.5-HP PMSM—initial training iteration.

in [5] to be robust to the mechanical parameters such as load torque.

In order to evaluate the effectiveness of the DRNN adaptation process, the system was trained offline using data from a 7.5 horsepower PMSM with stator resistance and inductance of $.12 \Omega$ and 3.2 H , respectively, and a voltage constant of $K_e = .166 \text{ v} - \text{s/r}$. The system was then trained online using a 2.5 horsepower motor with stator resistance and inductance of 1.35Ω and 1.3 H , respectively, and $K_e = .12 \text{ v} - \text{s/r}$. The position estimation performance is shown in Fig. 8 for the first on-line training iteration. After much additional online training, the rotor angle estimation error shown in Fig. 9 was achieved. This result demonstrates the principal advantage of the neural approach—machine operation can effectively be learned without accurate knowledge or need of machine parameters.

In Fig. 10, the robustness of the DRNN rotor position estimation technique to angular velocity estimation error is demonstrated. For this experiment, a ± 50 percent error in the estimated rotor velocity was intentionally introduced to the system. The

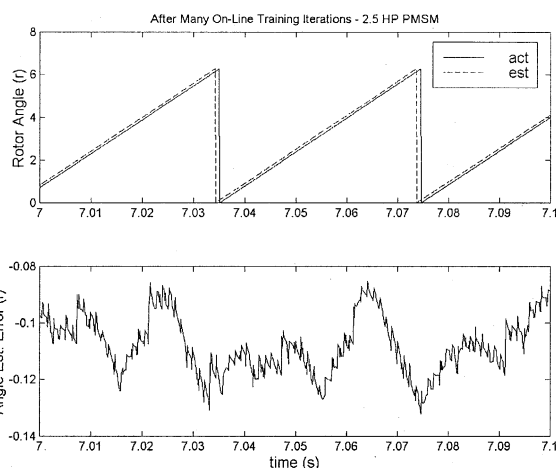


Fig. 9. Online training of 2.5-HP PMSM—after many training iterations.

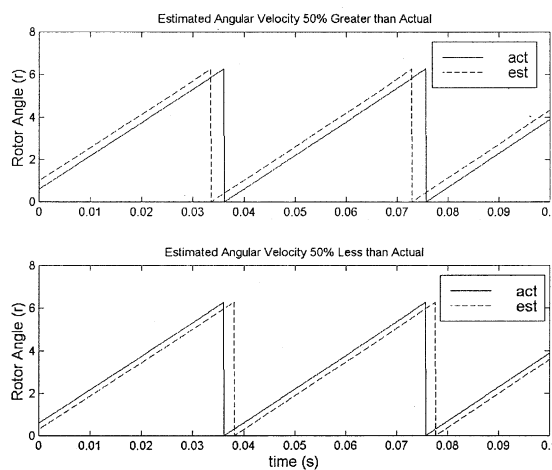


Fig. 10. NN estimation accuracy with velocity estimation error.

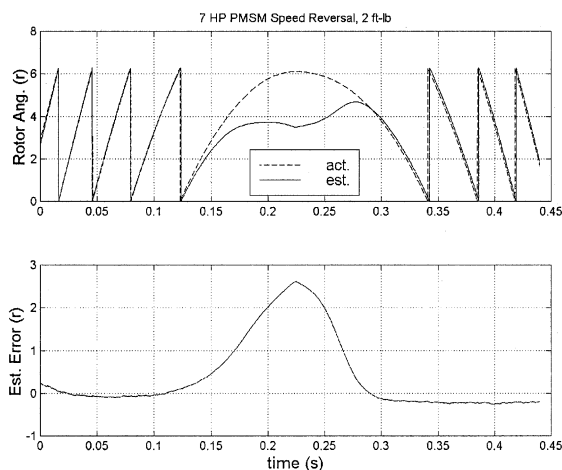


Fig. 11. NN estimation accuracy for speed reversal.

figure shows that, despite the exaggerated error in the angular velocity, the rotor position is still estimated with acceptable accuracy for many applications.

Finally, Fig. 11 shows the performance of the rotor position estimator during a speed reversal. Here, significant error is evident around the zero speed operation where the slope of the

rotor angle becomes zero. This is due to the well-known unobservability of rotor angle at zero speed because of the lack of developed stator voltage under those operating conditions. Sensorless operation at zero speed is known to be problematic, and thus, startup and speed reversals are often achieved through alternate strategies [10]–[13] while the estimator is effectively disabled.

V. CONCLUSIONS

A neural-based observer, whose architecture is patterned from the results of a model-based approach, was designed and applied to the rotor position estimation task for the PMSM. The DRNN was selected for the neural topology due to its dynamic mapping characteristics, fast convergence, and ease of implementation in real-time systems. Both the DRNN and model-based approach have demonstrated insensitivity to mechanical parameters such as load torque, inertia, and friction. In addition, the DRNN approach has shown the ability to learn the PMSM dynamics and robustness to the unavoidable drift and uncertainty of PMSM parameters. The advantages demonstrated by the DRNN approach are significant in general-purpose PMSM drives, where the end user may not know the PMSM parameters required by a model-based approach. In cases where machine parameters, saliency characteristics, and back emf waveshape are well defined, however, the model-based approach has produced superior rotor position estimation results in the experiments.

REFERENCES

- [1] R. Wu and G. Slemon, "A permanent magnet motor drive without a shaft sensor," *IEEE Trans. Ind. Applicat.*, vol. 27, pp. 1005–1011, Sept./Oct. 1991.
- [2] J. Moreira, "Indirect sensing for rotor flux position of permanent magnet AC motors over a wide speed range," *IEEE Trans. Ind. Applicat.*, vol. 32, pp. 1394–1401, Dec. 1996.
- [3] S. Ogasawara, K. Suzuki, and H. Akagi, "A sensorless brushless DC motor system," *Electrical Engineering in Japan*, vol. 12, no. 5, pp. 109–117, 1992.
- [4] L. Jones and J. Lang, "A state observer for the permanent magnet synchronous motor," *IEEE Trans. Ind. Electron.*, vol. 36, pp. 374–382, Aug. 1989.
- [5] T. D. Batzel and K. Y. Lee, "Slotless permanent magnet synchronous motor operation without a high resolution rotor angle sensor," *IEEE Trans. Energy Conversion*, vol. 15, pp. 366–371, Dec. 2000.

- [6] A. Kulkarni and M. Ehsani, "A novel position sensor elimination technique for the interior permanent magnet synchronous motor drive," *IEEE Trans. Ind. Applicat.*, vol. 28, pp. 144–150, Feb. 1992.
- [7] C. C. Ku and K. Y. Lee, "System identification and control using diagonal recurrent neural networks," in *Proc. 1992 Amer. Control Conf.*, vol. 1, June 1992, pp. 545–549.
- [8] —, "Diagonal recurrent neural networks for dynamic systems control," *IEEE Trans. Neural Networks*, vol. 6, pp. 144–156, Jan. 1995.
- [9] R. H. Park, "Two reaction theory of synchronous machines—Part I," *AIEE Transactions*, vol. 48, no. 2, pp. 716–730, 1929.
- [10] M. Schroedl, "Sensorless control of AC machines at low speed and standstill," in *Conf. Rec.—Ind. Applicat. Soc. Meeting*, vol. 1, 1996, pp. 270–277.
- [11] N. Matsui and T. Takeshita, "A novel starting method of sensorless salient-pole brushless motor," *Proc. Conf. Rec. 1994 Ind. Applicat. Soc. Annu. Meeting*, vol. 1, pp. 386–392, Oct. 1994.
- [12] T. Aihara, A. Toba, and T. Yanase, "Sensorless torque control of salient-pole synchronous motor at zero speed operation," in *IEEE Appl. Power Electron. Conf. Exposition*, vol. 2, 1997, pp. 715–720.
- [13] T. D. Batzel and K. Y. Lee, "Starting method for sensorless operation of slotless permanent magnet synchronous machines," in *Proc. IEEE Power Eng. Soc. Summer Meeting*, vol. 2, July 1999, pp. 1243–1247.



Todd D. Batzel received the B.S. and Ph.D. degrees in electrical engineering from the Pennsylvania State University, University Park, in 1984 and 2000, respectively, and the M.S. degree in electrical engineering from the University of Pittsburgh, Pittsburgh, PA, in 1989.

Currently, he is Assistant Professor of computer science at the Pennsylvania State University, Altoona. His research interests include machine controls, electric drives, power electronics, and artificial intelligence applications to control and

embedded control systems.



Kwang Y. Lee (F'01) received the B.S. degree in electrical engineering from Seoul National University, Korea, in 1964, the M.S. degree in electrical engineering from North Dakota State, Fargo, in 1968, and the Ph.D. degree in systems science from Michigan State University, East Lansing, in 1971.

Currently, he is a Professor of electrical engineering and is Director of Power Systems Control Laboratory at Pennsylvania State University, University Park. He has also been with Michigan State, Oregon State, and the University of Houston. His interests include power systems operation and planning, expert systems, and intelligent system applications to power systems.

Dr. Lee is an Editor of IEEE TRANSACTIONS ON NEURAL NETWORKS and IEEE TRANSACTIONS ON ENERGY CONVERSION. Dr. Lee is a Fellow of the IEEE.